Monodisperse behavior of polydisperse flows

Polanía, Oscar; Renouf, Mathieu; Cabrera, Miguel; Estrada, Nicolas; Azéma, Emilien

DOI
10.1103/PhysRevE.111.L043401

Publication date
2025

Document Version
Final published version

Published in
Physical Review E

Letter

Monodisperse behavior of polydisperse flows

Oscar Polanía,[1] Mathieu Renouf,[1,*] Miguel Cabrera,[2,†] Nicolas Estrada,[3,‡] and Emilien Azéma[1,4,5,§]

[1]*LMGC, Université de Montpellier, CNRS, Montpellier, France*

[2]*Department of Geoscience & Engineering, TU Delft, Delft, The Netherlands*

[3]*Department of Civil and Environmental Engineering, Universidad de los Andes, Bogotá, Colombia*

[4]*Department of Civil, Geological, and Mining Engineering, Polytechnique Montréal, Montréal, Canada*

[5]*Institut Universitaire de France (IUF), Paris, France*

(Received 17 November 2024; accepted 14 March 2025; published 14 April 2025)

Granular flows can occur under low inertia conditions, called the quasi-static regime, and extend to highly inertial systems, called the inertial regime. In the latter, granular flows, particularly those having a variety of grain sizes—property known as polydispersity—have not been extensively studied. Existing rheological laws for monodisperse flows effectively capture volume and friction variations across inertial ranges, assuming the grains diameter as the flow characteristic length. For polydisperse materials, this assumption is less intuitive, and rheological laws cannot be extended straightforwardly. In this work, we employed the Discrete Element Method to study granular flows across varying inertial levels, aiming to identify a physically based length scale that represents the grain scale for polydisperse flows. We show that the average branch length (i.e., distance between the centers of contacting grains) is a representative value of the material's grain size distribution, remaining nearly constant across the explored range of inertia. Moreover, we show that monodisperse and polydisperse flows follow common inertial volume and friction laws when the average branch length is considered as the characteristic length. The findings of this work propose a new perspective for understanding the characteristic length of granular flows, providing a comprehensive interpretation based on the grains contacts. They also permit to extend rheological laws, initially proposed for monodisperse flows, to polydisperse flows by considering the characteristic length scale as the average branch length. Finally, Our results are useful for choosing the characteristic length that controls large-scale flows where polydispersity plays an important role.

DOI: 10.1103/PhysRevE.111.L043401

Introduction. Granular flows are complex processes where grains interact through contacts that develop extensive and constantly evolving force networks [1]. These flows are involved in many scenarios and scales, from geophysical mass flows such as landslides, debris flows, pyroclastic flows, and snow avalanches to industrial processes like pharmaceuticals, food production, and construction [2]. Granular flows are processes where large deformations occur, reaching a state where plasticity develops and irreversible shear deformations begin to accumulate, while the material packing fraction ϕ and the effective friction μ fluctuate around approximately constant values.

In dry flows, the collective motion of grains and the macroscopic features, such as volume and strength, are governed by the system inertia. A dimensionless quantity, called the *Inertial number*, defined as

$$I = \frac{\dot{\gamma} d}{\sqrt{P/\rho}}, \tag{1}$$

has proven extremely useful for describing granular flows [3,4]. The inertial number I can be interpreted as the ratio between two time scales: the global deformation time $\tau_\gamma = 1/\dot{\gamma}$ and the confinement timescale $\tau_c = d/\sqrt{P/\rho}$. In Eq. (1), $\dot{\gamma}$, P, d, and ρ are the shear deformation rate, the confinement pressure, the characteristic diameter, and density of the grains, respectively. Granular flows can occur under low-inertia conditions, with long-lasting contacts in a quasi-static regime ($I \lesssim 10^{-3}$), and extend to highly inertial systems where grains interact through collisions and brief contacts in the so-called dense regime ($10^{-3} \lesssim I \lesssim 1$). For $I \gg 1$, granular flows are characterized by few grains in contact, interacting primarily through nearly instantaneous binary contacts [5,6].

Steady granular flows, from quasi-static to dense, follow a friction law $\mu(I)$ that works for the case of nearly monodisperse grains [7]. Moreover, the relevance of I can be extended to account for volumetric variations through a volume law $\phi(I)$, which captures the state changes of granular materials [8]. The laws $\mu(I)$ and $\phi(I)$ are well established within the granular materials community, being successfully used in a large set of studies on granular flows (for some examples, see [9–14]). In this inertial model, granular rheology depends on a characteristic length scale of the mechanics at the grain level and this length is the grains' diameter d [see Eq. (1)] [5,15,16].

Granular flows, and especially those involved in large-scale processes [17–19], consist of grains of different sizes, a property known as *polydispersity*. In polydisperse flows, defining a characteristic diameter d is not intuitive due to the wide range

*Contact author: mathieu.renouf@umontpellier.fr
†Contact author: m.a.cabrera@tudelft.nl
‡Contact author: n.estrada22@uniandes.edu.co
§Contact author: emilien.azema@umontpellier.fr

of grain sizes within the material's grain size distribution (GSD). This is a major concern, because, in order to straightforwardly extend $\mu(I)$ and $\phi(I)$ to polydisperse materials, it is needed to account for a length scale that characterises the flow. For quasi-static flows, different studies have shown that μ is independent of the polydispersity level [20–26], implicitly suggesting that μ at low I is independent of the characteristic length scale. Contrarily, for granular flows in the inertial regime, despite the efforts carried out in previous studies [27–35], the choice of a characteristic length is not yet well established within the community.

Our objective is to determine if there is a physically based length scale such that the laws $\phi(I)$ and $\mu(I)$, initially proposed for monodisperse flows, remain valid for polydisperse flows. To do this, we conducted three-dimensional numerical simulations using the Discrete Element Method (DEM) to study granular flows in a simple shear configuration. We studied samples with different polydispersity levels and systematically varied the system inertia across orders of magnitude, ranging from quasi-static to inertial (or dense) flows. We explored whether length scales obtained from the grains participating in the force contact network, such as the average branch length (i.e., the distance between the centers of contacting grains) or the average grain diameter, are representative of granular flows and if they can describe the flow macroscopic behavior.

Numerical tool and setup. The simulations conducted for this study were carried out using DEM of the type Non-Smooth Contact Dynamic (NSCD) [36]. The NSCD method updates grain positions based on a set of inequalities that relate the impulse and the local relative velocity, eliminating the need for elastic repulsion or friction smoothing. In polydisperse assemblies, regularized contact models require stiffness parameters that depend on grain size, leading to non-trivial calibration issues. In particular, the penetration allowed by such regularization does not scale uniformly with particle size, potentially introducing artificial effects. This issue may be critical in polydisperse granular flows where small grains can transiently reach high velocities, inducing spurious wave propagation that constrains the choice of time step. By formulating contact interactions through non-smooth constraints, NSCD avoids these challenges, making it a suitable approach for studying polydisperse granular systems. Simulations were done with the open source software LMGC90 developed in LMGC, Université de Montpellier, France [37].

We defined the polydispersity level as $\lambda = d_{\max}/d_{\min}$, where $d_{\max}$ and $d_{\min}$ represent the maximum and minimum grain diameters in the sample, and explored systems with $\lambda = [1.2, 4.0, 6.0, 8.0]$. With these levels of polydispersity, we studied granular assembles with initial packing fractions $\phi_0(\lambda) = [0.60, 0.67, 0.71, 0.78]$. Our samples were built within a box of dimensions $L_x = 15d_{50}$, $W_y = 8d_{50}$, and $H_z \sim 16d_{50}$ with $d_{50} = 1$ mm being the diameter holding the ∼50% of the cumulative mass and also representing the mean value between $d_{\min}$ and $d_{\max}$. We defined periodic boundaries in the XZ and YZ planes. In the XY planes, two rough clusters composed of grains with a diameter d_{50} impose the boundary conditions. A constant force $F_Z = \pm 22.5$ N is applied to the rough clusters, exerting a confinement pressure $P = F_Z/(L_x W_y)$, along with a constant horizontal velocity $\pm V_x$ (see Fig. 1). The velocity V_x was chosen to study granular flows within a range $I(d_{50}) \in [1 \times 10^{-4}, 5 \times 10^{-1}]$, with $d = d_{50}$ and $\dot{\gamma} = 2V_x/H_z$ [see Eq. (1)], allowing us to explore granular flows from quasi-static to dense regimes. In our simulations, gravity was set to zero; therefore, size segregation is not likely to occur (see Appendix A in the Supplemental Material for more details on the numerical setup [38] (including Refs. [39,40])).

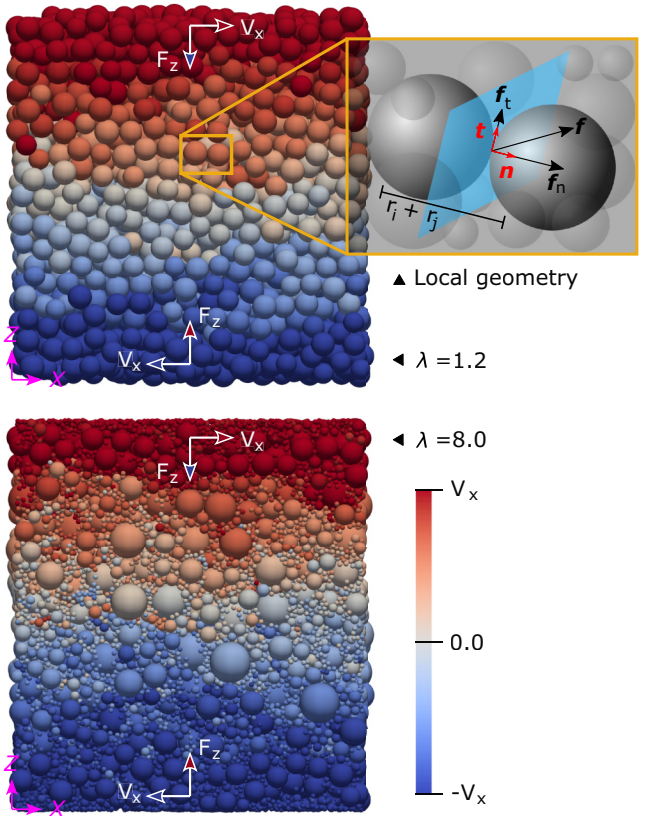

FIG. 1. Monodisperse ($\lambda = d_{\max}/d_{\min} = 1.2$) and polydisperse ($\lambda = 8$) samples during shearing. Bottom and top roughs clusters composed of spheres with diameter $d_{50} = 1$ mm impose constant force F_Z and velocity V_X. The color bar presents the grains velocity in the x axis. The zoom presents the local geometry of a contact, with $\boldsymbol{n}$, $\boldsymbol{t}$, $\boldsymbol{f}$, and r being the normal and tangential unit vectors, the contact force, and the radii of the grains in contact, respectively. The blue plane represents the tangential contact plane.

Macroscopic behavior. The agitation caused by increasing I provokes an expansion of the material, resulting in systems with a lower packing fraction ϕ. This is shown in Fig. 2(a). In our case, as in previous studies [4,9], the relationship between ϕ and I for monodisperse systems follows a linear trend. Specifically, for our results, this relationship is well described by $\phi(I) = \phi_0(a - bI)$, where ϕ_0 is the packing fraction in the quasistatic limit as $I \to 0$, and the constants a and b represent the initial sample dilatancy and the rate of inertial volume change, respectively. For all λ, ϕ consistently decreases with I, following approximately parallel trends that depend on the initial packing fraction ϕ_0. Hence, within the range of I explored in our study, the initially densest systems—those with the greatest λ—remain the densest after reaching the steady state. It is important to highlight that for larger I, when the

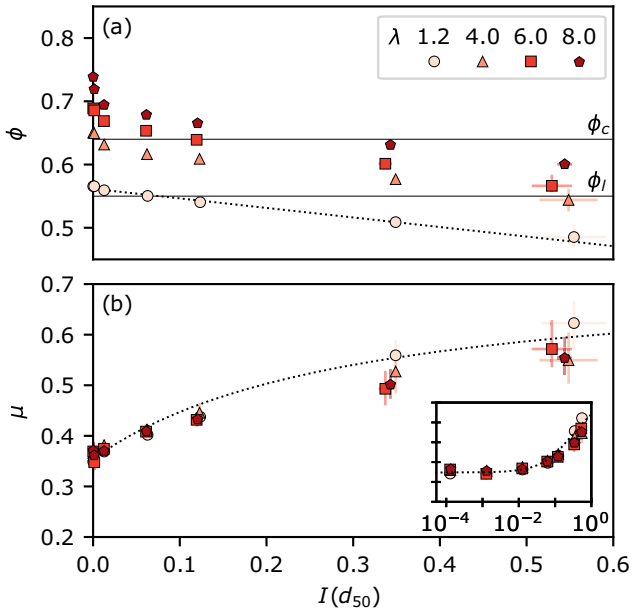

FIG. 2. (a) Packing fraction ϕ and (b) effective friction μ as functions of the inertial number $I(d_{50})$ for all polydispersity levels λ. In (a), the dotted line follows the inertial volume law $\phi(I) = \phi_0(0.93 - 0.25I)$ with $\phi_0 = 0.6$, and the horizontal lines present the reference values of a random loose packing $\phi_l = 0.55$ and a random close packing $\phi_c = 0.64$ of monodisperse spheres [41]. In (b), the dotted line is the friction law presented in Eq (2) with $\mu_s = 0.34$, $\mu_2 = 0.73$, and $I_0 = 0.28$. The inset presents the same information in semi-log scale.

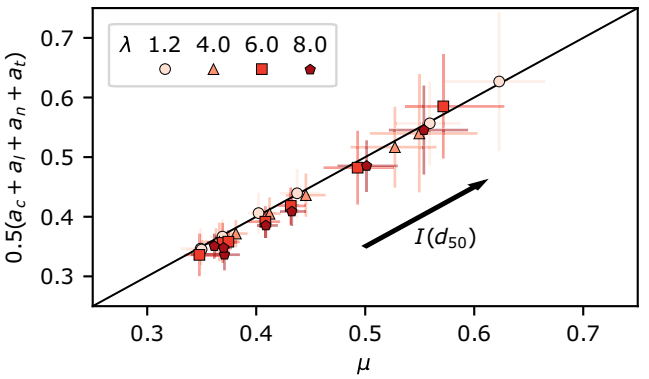

FIG. 3. Correlation between the effective friction μ and the addition of the fabric (a_c and a_l) and force (a_n and a_t) anisotropies. The markers shape stands for the polydispersity level λ, and colors, from the darkest to the lightest, represent the increase of the inertial number $I(d_{50}) \sim [10^{-4}, 0.5]$. The line represents the 1 : 1 ratio, and the error bars represent the variability in the steady state.

ϕ is less than the critical for which rate-independent components of the stresses arise [42], it is necessary to use different volume laws, such as a power function [43,44].

The other macroscopic feature that we evaluated, the macroscopic friction coefficient μ, exhibits a systematic increase with I, calculated with d_{50} according to Eq. (1), for all values of λ. This is shown in Fig. 2(b) [see Appendix B in the Supplemental Material for the computation of μ [38] (including Ref. [45])]. The increase in μ occurs because an increase in inertia causes the grains to interact through short-lasting contacts, leading to high linear momentum transfer and large contact force magnitudes [46–49]. In our case, μ for monodisperse samples agrees with the inertial friction law

$$\mu = \mu_s + \frac{\mu_2 + \mu_s}{I_0/I + 1}, \tag{2}$$

where μ_s is the friction coefficient when $I \to 0$, μ_2 is a saturation friction value for large I, and I_0 is a material constant [7]. This law, originally proposed for monodisperse flows, describes well the behavior of polydisperse samples for $I \lesssim 0.1$, allowing us to confirm and claim that μ remains independent of λ for a broad range of I [32]. However, for $I > 0.1$, μ for polydisperse flows deviates from the trend, exhibiting an apparent decrease in effective friction compared to monodisperse flows.

System micromechanics. From a micro-mechanical perspective, the increase in $\mu(I)$ is produced by an increase in the system disorder, expressed as the anisotropies of the contact and force distributions [50,51]. Specifically, the quantities that build μ in a granular material are the anisotropies of contact orientation a_c, branch length a_l, normal forces a_n, and tangential forces a_t [20,22,52]. Generally speaking, a_c and a_l describe the geometric organization of the granular structure. *ac* characterizes the spatial connectivity of contacts, while a_l, which is more sensitive to the grain size distribution, captures the spatial arrangement of the grain positions. On the other hand, a_n and a_t describe the force network. a_n quantifies the directional distribution of normal forces, while a_t reflects the spatial organization and mobilization of friction forces within the material. These anisotropies, originally proposed from the polar distributions of contacts and forces [50], can be also obtained using the fabric and force tensors [53] [see Eqs. (C1) and (C2) in the Appendix [38]).

The addition of fabric and force anisotropies is equivalent to the macroscopic friction of granular materials as $\mu \simeq (a_c + a_l + a_n + a_t)/2$ [50]. This correlation has been shown to work accurately for monodisperse flows within quasi-static and inertial regimes [51], as well as in polydisperse flows in a quasi-static regime [20,22,25,52]. Here, we extend the accuracy of this friction-anisotropy correlation and evidence that it holds true for polydisperse flows even in the dense regime, as shown in Fig. 3. This result allows us to rely on the individual anisotropies to understand the relative decay of μ for polydisperse flows compared to monodisperse ones [see Fig. 2(b)].

A close look at the anisotropies variation with I reveals that, in the quasi-static regime $I \lesssim 10^{-3}$, μ is independent of λ due to the compensation between a_c and a_n. Then, for larger I, an increase in μ is mainly due to an increase in a_c, while the other anisotropies remain approximately constant [51]. This increase occurs more rapidly in monodisperse flows, leading to a faster growth in the macroscopic friction when compared to polydisperse flows with a common inertial number $I(d_{50})$ [see the individual fabric and force anisotropies as a function of I in Fig. 2 in Appendix B of [38] (including Refs. [54,55])]. However, a strong assumption underlies these observations, namely the use of d_{50} as the characteristic length scale. Thus,

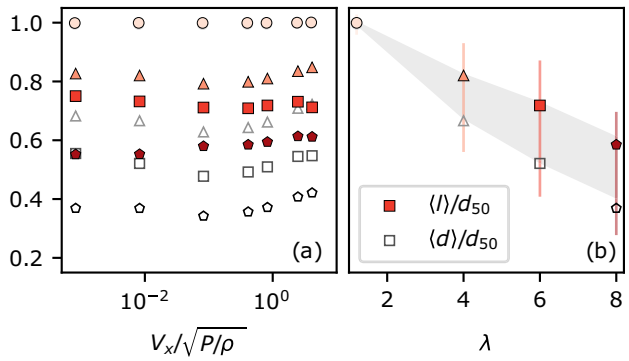

FIG. 4. Variation of the mean branch length $\langle l\rangle$ (filled markers) and the mean grain diameter of the grains with active contacts $\langle d\rangle$ (empty markers) as functions of (a) $V_x/\sqrt{P/\rho}$ and (b) λ. In (b), the results present $\langle l\rangle$ and $\langle d\rangle$ averaged for each GSD across all V_x. The vertical error bars (included only for $\langle l\rangle$) represent the minimum and maximum first and third quartiles, respectively, obtained for the data series of each λ. The grey region is delimited by the Sauter-mean diameter $d_S = \sum_i^N d_i^3 / \sum_i^N d_i^2$ (upper limit) and the root-mean-cubed diameter $d_{\rm rmc} = \left(\sum_i^N d_i^3/N\right)^{1/3}$ (lower limit) of the GSD. Makers shape (see legend of Fig. 2) and color represent the polydispersity level (with the lightest and the darkest being $\lambda = 1.2$ and 8.0, respectively).

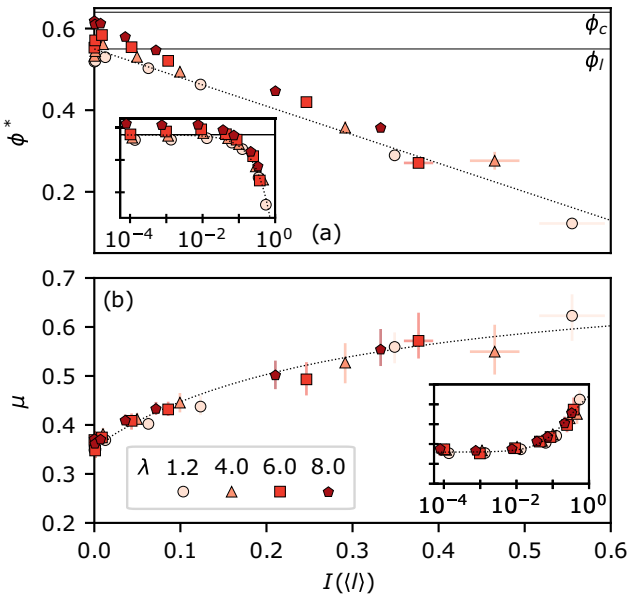

FIG. 5. (a) Load-carrying packing fraction ϕ^* and (b) macroscopic friction μ as functions of the inertial number I considering $d = \langle l\rangle$ [see Eq. (1)] for all polydispersity levels λ. In (a), the dashed line follows the inertial law $\phi^*(I) = \phi_l - 0.7I$ with $\phi_l = 0.55$ [41]. In (b), the dotted line is the friction law presented in Eq. (2) with $\mu_s = 0.34$, $\mu_2 = 0.73$ and $I_0 = 0.28$. The insets present the same information in semi-log scale.

an important question arises: Is d_{50} actually a good choice for computing the inertial number I?

Characteristic length scale. The diameter d is a first order coefficient for computing I, and it is the only variable in it that could account for polydispersity. In the definition of I, d is interpreted as the effective displacement necessary for a local relaxation in the confinement time scale τ_c. Thus, this displacement defines the length scale for I. For monodisperse systems, the branch length l, or the distance between the centers of contacting grains (see inset in Fig. 1), is equal to d. While in polydisperse systems, due to the variety of grain sizes, one has a distribution of l and d. Therefore, with the aim of identifying the representative length scale in the stress contribution [56], we find that the averaged values $\langle l\rangle$ and $\langle d\rangle$—the latter restricted to grains participating in the force network—remain nearly constant over a wide range of flow velocities. This is shown in Fig. 4(a). This result is notable because it shows that both $\langle l\rangle$ and $\langle d\rangle$ can be considered characteristic length scales, being a sort of fingerprint of the system GSD. Since we use linear volume GSDs, both $\langle l\rangle$ and $\langle d\rangle$ decrease with the polydispersity level λ, as the GSD widening implies an increase of the number of small grains in the system. A notable observation is that $\langle l\rangle$ and $\langle d\rangle$, which are exclusively obtained from the grains participating in the force network, evolve similarly to those of the Sauter-mean d_S, equivalent diameter that accounts for the volume-to-surface ratio [57], and the Root-mean-cubed diameter $d_{\rm rmc}$, respectively [see Fig. 4(b)]. These equivalent diameters, obtained from the GSD, have been previously proposed as characteristic length scales of polydisperse systems [27,30].

The length scales $\langle l\rangle$ and $\langle d\rangle$ are values obtained from the contact network, and it is not possible to obtain these values directly in natural or industrial granular flows. However, a relevant aspect of the result presented in Fig. 4(b) is the potential to estimate these values because we observe a strong correlation between them and the average diameters $d_{\rm rmc}$ and d_S that can be computed from the GSD. Therefore, this result provides a practical way of obtaining two system length scales, $\langle l\rangle$ and $\langle d\rangle$, in applied contexts (e.g., geophysical or industrial processes) and offers a comprehensive interpretation of their physical meaning [58].

The average branch length $\langle l\rangle$, always larger than the average diameter $\langle d\rangle$, seems like a length scale that could better describe a polydisperse granular flow. This statement stems from the following idea: If the stress tensor $\boldsymbol{\sigma}$(see Eq. (B1) in the Appendix and, consequently, the effective friction μ are computed from the branch length l, then could the average branch length $\langle l\rangle$ serve as a suitable length scale for computing the inertial number I in polydisperse flows? One might hypothesize that rather than considering a polydisperse flow as a network of branches with varying lengths, a polydisperse flow behaves like a monodisperse one with grains of equivalent size $\langle l\rangle$. If this hypothesis holds true, the inertial number of polydisperse flows should be computed as $I(d = \langle l\rangle)$.

A common behavior with $\langle l\rangle$ as characteristic length. Up to this point, we have discussed the relevance of the grains in contact for obtaining a characteristic local length scale for computing I. Additionally, by definition, the effective friction coefficient μ exclusively depends on the grains actively participating in the force network. Therefore, following the same logic, we also compute the *effective* packing fraction ϕ^* [59], that stands for the grains' volume that participate in the contact network. Figure 5(a) shows ϕ^* as a function of $I(\langle l\rangle)$ for all polydispersity levels λ.

Despite the scatter at low inertial numbers due to the greater connectivity in polydisperse materials, it can be seen that most data tend to collapse onto the common trend $\phi^*(I) \propto I$. It is important to highlight that all grains, whether floating or in contact, are part of a force network that evolves dynamically, with grains continuously entering and leaving. Nevertheless, this result reveals that, over a long-term average, the effective volume of grains participating in the contact network appears to be independent of λ and instead relies on I.

Additionally, we evidence that all granular flows, regardless of their GSD, follow the inertial friction law introduced in Eq. (2) when the flow characteristic length scale is considered as $\langle l \rangle$. This is presented in Fig. 5(b). These results are outstanding because they show that $\mu(I)$ and $\phi^*(I)$ for polydisperse flows can be computed using exactly the same laws as for monodisperse flows, thus reducing the complexity of these processes. The key ingredient is simply to correctly set the characteristic length scale as one that is truly representative of the grains taking part in the force-carrying backbone of the system. Through this result, we prove that $\langle l \rangle$ is a reliable and physically based length scale for computing the flow inertial number $I(\langle l \rangle)$. Moreover, we show that d_S is a good candidate when micro-mechanical information is not available [see Fig. 4(b)].

A table summarizing the simulations conducted and the results supporting our conclusions can be found in the Supplemental Material [38].

Conclusions. In summary, we conducted an extensive numerical work with DEM, studying granular flows with various levels of polydispersity and covering a broad range of inertial numbers I, within quasistatic and inertial regimes. We showed that both the average branch length $\langle l \rangle$ and the average diameter $\langle d \rangle$, the latter restricted to grains participating in the force network, are length scales that remain nearly constant across the range of inertial numbers we evaluated. By using $\langle l \rangle$ as a characteristic length scale, we find that for granular flows with different polydispersity levels the effective friction coefficient μ is well described by the inertial law that was initially proposed for monodisperse granular materials. This confirms that the average center-to-center distance is a much better choice for defining a characteristic length scale than the average diameter. In a certain way, these results show that, when computing the inertial number, it is possible to assume polydisperse granular flows as an equivalent monodisperse collection of grains having a diameter $d = \langle l \rangle$. If $\langle l \rangle$ is unavailable, as is the case of field applications or experimental observations, we suggest using the Sauter-mean diameter d_S derived from the grain size distribution (GSD) as the characteristic length scale, as it demonstrated a strong correlation with $\langle l \rangle$. The average branch length $\langle l \rangle$, as an input parameter for granular materials, may prove useful for selecting the characteristic length scale or choosing the size of elementary volume elements in continuum simulations of polydisperse granular flows, as well as in scaling laws for the mobility of landslides that require a characteristic grain size. Finally, we find that the load-carrying packing fraction ϕ^* (i.e., the volume of grains that participate in the force network) is independent of polydispersity and only depends on the inertial number.

Our results provide a comprehensive interpretation of the length scale to be considered in polydisperse granular flows; however, our study exclusively explored linear GSDs. Further research could focus on extending or proving our conclusions for other types of GSD, like fractal distributions. Additionally, further research could include gravity to account for segregation phenomena, in order to understand how the characteristic length scale of polydisperse flows evolves over time and what are the implications for macroscopic friction and packing fraction.

Acknowledgment. Simulations were carried out using the High-Performance Computing Platform MESO@LR of Université de Montpellier.

[1] F. Radjai, Modeling force transmission in granular materials, C. R. Phys. **16**, 3 (2015).

[2] D. J. Jerolmack and K. E. Daniels, Nat. Rev. Phys. **1**, 716 (2009).

[3] I. Iordanoff and M. M. Khonsari, Granular lubrication: Toward an understanding of the transition between kinetic and quasi-fluid regime, J. Tribol. **126**, 137 (2004).

[4] F. da Cruz, S. Emam, M. Prochnow, J.-N. Roux, and F. Chevoir, Rheophysics of dense granular materials: Discrete simulation of plane shear flows, Phys. Rev. E **72**, 021309 (2005).

[5] G. MiDi, On dense granular flows, Eur. Phys. J. E **14**, 341 (2004).

[6] D. Berzi, On granular flows: From kinetic theory to inertial rheology and nonlocal constitutive models, Phys. Rev. Fluids **9**, 034304 (2024).

[7] P. Jop, Y. Forterre, and O. Pouliquen, A constitutive law for dense granular flows, Nature (London) **441**, 727 (2006).

[8] Y. Forterre and O. Pouliquen, Flows of dense granular media, Annu. Rev. Fluid Mech. **40**, 1 (2008).

[9] O. Pouliquen and Y. Forterre, A non-local rheology for dense granular flows, Philos. Trans. R. Soc. A **367**, 5091 (2009).

[10] L. Staron, P.-Y. Lagrée, and S. Popinet, The granular silo as a continuum plastic flow: The hour-glass vs the clepsydra, Phys. Fluids **24**, 103301 (2012).

[11] P.-Y. Lagrée, L. Staron, and S. Popinet, The granular column collapse as a continuum: validity of a two-dimensional navier–stokes model with a μ(i)-rheology, J. Fluid Mech. **686**, 378 (2011).

[12] A. Abramian, L. Staron, and P.-Y. Lagrée, The slumping of a cohesive granular column: Continuum and discrete modeling, J. Rheol. **64**, 1227 (2020).

[13] S. Deboeuf and A. Fall, Cohesion and aggregates in unsaturated wet granular flows down a rough incline, J. Rheol. **67**, 909 (2023).

[14] G. Yang, S. Yang, L. Jing, C. Kwok, and Y. Sobral, Efficient lattice Boltzmann simulation of free-surface granular flows with μ(i)-rheology, J. Comput. Phys. **479**, 111956 (2023).
[15] K. Kamrin, K. M. Hill, D. I. Goldman, and J. E. Andrade, Advances in modeling dense granular media, Annu. Rev. Fluid Mech. **56**, 215 (2024).
[16] P. Shekari, B. Marks, and P. Rognon, Size of heterogeneous deformations in sheared granular flows, Phys. Rev. Fluids **8**, 124301 (2023).
[17] L. F. Prada-Sarmiento, M. A. Cabrera, R. Camacho, N. Estrada, and A. M. Ramos-Cañón, The mocoa event on march 31 (2017): Analysis of a series of mass movements in a tropical environment of the Andean-Amazonian Piedmont, Landslides **16**, 2459 (2019).
[18] R. Kostynick, H. Matinpour, S. Pradeep, S. Haber, A. Sauret, E. Meiburg, T. Dunne, P. Arratia, and D. Jerolmack, Rheology of debris flow materials is controlled by the distance from jamming, Proc. Natl. Acad. Sci. USA **119**, e2209109119 (2022).
[19] O. Polanía, N. Estrada, E. Azéma, M. Renouf, and M. Cabrera, Polydispersity effect on dry and immersed granular collapses: an experimental study, J. Fluid Mech. **983**, A40 (2024).
[20] C. Voivret, F. Radjaï, J.-Y. Delenne, and M. S. El Youssoufi, Multiscale force networks in highly polydisperse granular media, Phys. Rev. Lett. **102**, 178001 (2009).
[21] N. Estrada, Effects of grain size distribution on the packing fraction and shear strength of frictionless disk packings, Phys. Rev. E **94**, 062903 (2016).
[22] D. Cantor, E. Azéma, P. Sornay, and F. Radjai, Rheology and structure of polydisperse three-dimensional packings of spheres, Phys. Rev. E **98**, 052910 (2018).
[23] S. Zhao, J. Zhao, and N. Guo, Universality of internal structure characteristics in granular media under shear, Phys. Rev. E **101**, 012906 (2020).
[24] Y. Zhu, Z. Nie, J. Gong, J. Zou, L. Zhao, and L. Li, An analysis of the effects of the size ratio and fines content on the shear behaviors of binary mixtures using dem, Comput. Geotech. **118**, 103353 (2020).
[25] D. Cantor, E. Azéma, and I. Preechawuttipong, Microstructural analysis of sheared polydisperse polyhedral grains, Phys. Rev. E **101**, 062901 (2020).
[26] O. Polanía, M. Cabrera, M. Renouf, E. Azéma, and N. Estrada, Grain size distribution does not affect the residual shear strength of granular materials: An experimental proof, Phys. Rev. E **107**, L052901 (2023).
[27] S. Dahl, R. Clelland, and C. Hrenya, Three-dimensional, rapid shear flow of particles with continuous size distributions, Powder Technol. **138**, 7 (2003).
[28] P. G. Rognon, J.-N. Roux, M. Naaïm, and F. Chevoir, Dense flows of bidisperse assemblies of disks down an inclined plane, Phys. Fluids **19**, 058101 (2007).
[29] M. Otsuki and H. Hayakawa, Critical behaviors of sheared frictionless granular materials near the jamming transition, Phys. Rev. E **80**, 011308 (2009).
[30] Y. Gu, A. Ozel, and S. Sundaresan, Rheology of granular materials with size distributions across dense-flow regimes, Powder Technol. **295**, 322 (2016).
[31] E. C. P. Breard, J. Dufek, L. Fullard, and A. Carrara, The basal friction coefficient of granular flows with and without excess pore pressure: Implications for pyroclastic density currents, water-rich debris flows, and rock and submarine avalanches, J. Geophys. Res. B: Solid Earth **125**, e2020JB020203 (2020).
[32] M. Cabrera and N. Estrada, Is the grain size distribution a key parameter for explaining the long runout of granular avalanches? J. Geophys. Res. B: Solid Earth **126**, e2021JB022589 (2021).
[33] E. C. P. Breard, L. Fullard, and J. Dufek, Rheology of granular mixtures with varying size, density, particle friction, and flow geometry, Phys. Rev. Fluids **9**, 054303 (2024).
[34] A. Shi, G. Yang, C. Kwok, and M. Jiang, Enhanced mobility of granular avalanches with fractal particle size distributions: Insights from discrete element analyses, Earth Planet. Sci. Lett. **642**, 118835 (2024).
[35] Z. Ding, W. Hu, C. Chang, Y. Li, and G. Wang, Shear behaviors of confined flow: Insights for understanding the influences of fractal particle size distribution on high mobility of granular flows, Geophys. Res. Lett. **51**, e2024GL108956 (2024).
[36] M. Jean, The non-smooth contact dynamics method, Comput. Methods Appl. Mech. Eng. **177**, 235 (1999).
[37] F. Dubois and M. Jean, The non smooth contact dynamic method: Recent LMGC90 software developments and application, *Analysis and Simulation of Contact Problems*, edited by P. Wriggers and U. Nackenhorst (Springer Berlin Heidelberg, 2006), pp. 375–378.
[38] See Supplemental Material at http://link.aps.org/supplemental/10.1103/PhysRevE.111.L043401 for a table summarizing the simulations conducted, the results supporting our conclusions and the Appendix.
[39] C. Voivret, F. Radjaï, J.-Y. Delenne, and M. S. El Youssoufi, Space-filling properties of polydisperse granular media, Phys. Rev. E **76**, 021301 (2007).
[40] P. Mutabaruka, M. Taiebat, R. J.-M. Pellenq, and F. Radjai, Effects of size polydispersity on random close-packed configurations of spherical particles, Phys. Rev. E **100**, 042906 (2019).
[41] G. D. Scott, Packing of spheres: Packing of equal spheres, Nature (London) **188**, 908 (1960).
[42] S. Chialvo, J. Sun, and S. Sundaresan, Bridging the rheology of granular flows in three regimes, Phys. Rev. E **85**, 021305 (2012).
[43] I. Srivastava, L. E. Silbert, G. S. Grest, and J. B. Lechman, Viscometric flow of dense granular materials under controlled pressure and shear stress, J. Fluid Mech. **907**, A18 (2021).
[44] P.-E. Peyneau and J.-N. Roux, Frictionless bead packs have macroscopic friction, but no dilatancy, Phys. Rev. E **78**, 011307 (2008).
[45] L. Rothenburg, *Micromechanics of idealized granular systems*, Ph.D. Thesis, Carleton University, 1981.
[46] G. Lois, A. Lemaître, and J. M. Carlson, Spatial force correlations in granular shear flow. I. Numerical evidence, Phys. Rev. E **76**, 021302 (2007).
[47] D. Bonamy, F. Daviaud, L. Laurent, M. Bonetti, and J. P. Bouchaud, Multiscale clustering in granular surface flows, Phys. Rev. Lett. **89**, 034301 (2002).
[48] O. Pouliquen, Velocity correlations in dense granular flows, Phys. Rev. Lett. **93**, 248001 (2004).
[49] M. Macaulay and P. Rognon, Inertial force transmission in dense granular flows, Phys. Rev. Lett. **126**, 118002 (2021).

[50] L. Rothenburg and R. J. Bathurst, Analytical study of induced anisotropy in idealized granular materials, Géotechnique **39**, 601 (1989).

[51] E. Azéma and F. Radjaï, Internal structure of inertial granular flows, Phys. Rev. Lett. **112**, 078001 (2014).

[52] E. Azéma, F. Radjai, and F. Dubois, Packings of irregular polyhedral particles: Strength, structure, and effects of angularity, Phys. Rev. E **87**, 062203 (2013).

[53] F. Radjai, D. E. Wolf, M. Jean, and J.-J. Moreau, Bimodal character of stress transmission in granular packings, Phys. Rev. Lett. **80**, 61 (1998).

[54] M. S. Basson, A. Martinez, and J. T. DeJong, Dem simulations of the liquefaction resistance and post-liquefaction strain accumulation of coarse-grained soils with varying gradations, Comput. Geotech. **174**, 106649 (2024).

[55] Y. Li, Y. Dong, H. Jiang, and Z. Shi, Exploring the micromechanical origin of shear response in granular materials induced by size non-uniformity, Granular Matter **26**, 100 (2024).

[56] D. Liu, C. O'Sullivan, and J. A. H. Carraro, The influence of particle size distribution on the stress distribution in granular materials, Géotechnique **73**, 250 (2023).

[57] P. B. Kowalczuk and J. Drzymala, Physical meaning of the sauter mean diameter of spherical particulate matter, Part. Sci. Technol. **34**, 645 (2016).

[58] R. T. Cerbus, L. Brivady, T. Faug, and H. Kellay, Granular scaling approach to landslide runout, Phys. Rev. Lett. **132**, 254101 (2024).

[59] N. Estrada, A. Taboada, and F. Radjaï, Shear strength and force transmission in granular media with rolling resistance, Phys. Rev. E **78**, 021301 (2008).